Position and Velocity Navigation Systems for Unmanned Vehicles

Pedro Batista, *Student Member, IEEE*, Carlos Silvestre, *Member, IEEE*, and Paulo Oliveira, *Member, IEEE*

***Abstract*—This brief presents a new observer synthesis methodology for a class of kinematic systems with application to the estimation of linear motion quantities of mobile platforms (position and linear velocity), in three dimensions, that: 1) presents globally exponentially stable (GES) error dynamics, which are also input-to-state stable (ISS) with respect to angular quantities; 2) minimizes the $\mathcal{L}_2$ induced norm from a generalized disturbance input to a performance variable; 3) provides a systematic design procedure, based upon robust control theory results, that allows for the use of frequency weights to shape the dynamic response of the observer. A practical application is presented, in the field of ocean robotics, that demonstrates the potential and usefulness of the proposed design methodology and simulation results are included that illustrate the observer achievable performance in the presence of both extreme environmental disturbances and realistic sensors' noise.**

***Index Terms*—Estimation, navigation, robotics, time-varying observers, underwater vehicles.**

I. Introduction

THE design of Navigation and Positioning Systems plays a key role in the development of a large variety of mobile platforms for land, air, space, and marine applications. In the domain of marine research, for instance, the quality of the navigation data is a fundamental requirement in applications that range from ocean sonar surveying to ocean data acquisition (salinity, temperature, etc.) or sample collection (microbial organisms, sediments, etc.), as the acquired data sets should be properly georeferenced with respect to a given mission reference point. For control purposes, other quantities such as the attitude of the vehicle and/or the linear and angular velocities are also commonly required. This brief presents the design and performance evaluation of a time-varying globally exponentially stable (GES) observer for a class of kinematic systems with application to the estimation of linear quantities in Integrated Navigation Systems for mobile platforms.

To tackle this class of problems several approaches have been proposed in the literature. In [1] a GES nonlinear control law is presented for ships, in 2-D, which includes a nonlinear observer to provide the state variables of the vehicle. This observer relies on the vehicle dynamics but, as discussed in [2], it does not apply to unstable ships. In [2], a solution to an extended class of ships is proposed requiring only stable surge dynamics. In [3], a globally exponentially stable (GES) observer for ships (in 2-D) that includes features such as wave filtering and bias estimation is presented and in [4] an extension to this result with adaptive wave filtering is available. An alternative filter was proposed in [5] where the problem of estimating the velocity and position of an autonomous vehicle in 3-D was solved by resorting to special bilinear time-varying complementary filters. A passivity-based controller-observer design for robots with n degrees-of-freedom is proposed in [6] and a sliding mode observer for robotic manipulators is reported in [7]. The development of nonlinear observers for Euler–Lagrange systems has been addressed in [8] and [9]. More recently, a pair of co-working nonlinear Luenberger GES observers for aerial unmanned vehicles (AUVs), in 3-D, was proposed in [10], which also elaborates on the destabilizing Coriolis and centripetal forces and moments. However, this last approach assumes, among others, limited pitch angles. A nonlinear observer for a single degree-of-freedom decoupled underwater vehicle model can be found in [11], where the authors also present experimental results. General drawbacks of the previously mentioned results include the absence of systematic tuning procedures and the inherent limitations of the vehicle dynamic models, which are seldom known in full detail and may be subject to variations over time.

The main contribution of this brief is a new observer design methodology for a class of kinematic systems with application to the estimation of linear quantities (position, linear velocity, and ocean current) in Integrated Navigation Systems that:

1) presents globally exponentially stable error dynamics which are also input-to-state stable with respect to angular quantities;
2) minimizes the $\mathcal{L}_2$ induced norm from a generalized disturbance input to a performance variable;
3) provides a systematic design procedure based upon the latest robust control theory results, that allows for the use of frequency weights to shape the dynamic response of the observer.

At the core of the proposed methodology, there is a time-varying orthogonal coordinate transformation that renders the observer error dynamics linear time invariant (LTI). The problem is then formulated as a virtual control design problem which is solved by resorting to the standard $\mathcal{H}_\infty$ output feedback control synthesis technique. This method was preferred since it minimizes the $\mathcal{L}_2$ induced norm from a generalized disturbance input to a performance variable, which allows for the use of frequency weights in the design to shape the frequency response of the observer.

The general observer setup presented in the brief is suitable for the estimation of a large variety of linear motion quantities in Strapdown Integrated Navigation Systems for different types of vehicles and robotic platforms, depending on the sensor suite that is considered. For aerial, ground, or surface marine vehicles typical solutions arise from the use of the Global Positioning System (GPS), Doppler radars, and/or accelerometers, coupled

Manuscript received February 19, 2008. Manuscript received in final form April 28, 2008. First published March 06, 2009; current version published April 24, 2009. Recommended by Associate Editor F. Caccavale. This work was supported by Fundação para a Ciência e a Tecnologia (ISR/IST plurianual funding), by Project PTDC/MAR/64546/2006-OBSERVFLY, and by the project PDCT/MAR/55609/2004-RUMOS. The work of P. Batista was supported by a Ph.D. Student Scholarship from the POCTI Programme of FCT, SFRH/BD/24862/2005.

The authors are with the Institute for Systems and Robotics, Instituto Superior Técnico, 1049-001 Lisboa, Portugal (e-mail: pbatista@isr.ist.utl.pt; cjs@isr.ist.utl.pt; pjcro@isr.ist.utl.pt).

Digital Object Identifier 10.1109/TCST.2008.2001770

with Attitude and Heading Reference Systems (AHRS). For underwater vehicles Ultra-Short Baseline (USBL) accoustic positioning systems, Doppler velocity logs, and/or accelerometers lead to similar navigation solutions. An application of the proposed observer design technique is presented to estimate linear quantities in Integrated Navigation Systems for underwater vehicles. To describe the vehicle tridimensional motion the proposed observers rely on pure kinematic models. This class of models, expressed in the inertial coordinate system, has been widely used by the Navigation community, see [12] and the references therein. The present solution departs from previous approaches as it considers the rigid-body kinematics expressed in body-fixed coordinates, which is particularly suitable for direct application in strapdown navigation systems. This brief builds on previous work by the authors that can be found in [13] and [14], where a globally stable ocean current observer was designed to feed a nonlinear sensor-based integrated guidance and control law.

This brief is organized as follows. The theoretical results behind the proposed solutions are developed in Section II, including the observer design methodology and the derivation of several important properties. A relevant application in the field of ocean robotics, namely the estimation of unknown ocean currents, is presented in Section III, and simulation results are included that illustrate the achievable performance in the presence of extreme environmental disturbances and realistic noise of the sensors. Finally, Section IV summarizes the main contributions of this brief.

II. Theoretical Background

This section presents the design of an observer for a class of kinematic systems and the derivation of several properties of the proposed solution. The class of kinematic systems is introduced in Section II-A. Afterwards, the observer is developed in Section II-B. Section II-C presents some properties of the proposed solution. Throughout this brief the symbol $\mathbf{0}_{n\times m}$ denotes an $n \times m$ matrix of zeros, $\mathbf{I}_n$ an identity matrix with dimension $n \times n$, and $\mathrm{diag}(\mathbf{A}_1, \ldots, \mathbf{A}_n)$ a block diagonal matrix. When the dimensions are omitted the matrices are assumed to be of appropriate dimensions.

A. System Dynamics

Consider the class of dynamic systems

$$\begin{cases} \dot{\boldsymbol{\eta}}_1 = \mathbf{f}_1 + \gamma_1 \boldsymbol{\eta}_2 \\ \dot{\boldsymbol{\eta}}_2 = \mathbf{f}_2 + \gamma_2 \boldsymbol{\eta}_3 - \mathbf{S}(\boldsymbol{\omega})\boldsymbol{\eta}_2 \\ \cdots \\ \dot{\boldsymbol{\eta}}_{N-1} = \mathbf{f}_{N-1} + \gamma_{N-1}\boldsymbol{\eta}_N - \mathbf{S}(\boldsymbol{\omega})\boldsymbol{\eta}_{N-1} \\ \dot{\boldsymbol{\eta}}_N = \mathbf{f}_N - \mathbf{S}(\boldsymbol{\omega})\boldsymbol{\eta}_N \\ \boldsymbol{\psi} = \boldsymbol{\eta}_1 \end{cases} \tag{1}$$

where $\boldsymbol{\eta}_i = \boldsymbol{\eta}_i(t) \in X_i \subseteq \mathbb{R}^3, i = 1, \ldots, N$ are the system states, $\boldsymbol{\psi} = \boldsymbol{\psi}(t)$ is the system output, $\mathbf{f}_i = \mathbf{f}_i(t), i = 1, \ldots, N$, are known smooth functions of time, $\boldsymbol{\omega} = \boldsymbol{\omega}(t)$ is also a smooth function of time, $\gamma_i, i = 1, \ldots, N-1$, represents nonzero scalar constants, and $\mathbf{S}(\boldsymbol{\omega})$ is a skew-symmetric matrix that verifies $\mathbf{S}(\mathbf{a})\mathbf{b} = \mathbf{a} \times \mathbf{b}$, with $\times$ denoting the cross product, and that satisfies $\dot{\mathbf{R}}(t) = \mathbf{R}(t)\mathbf{S}(\boldsymbol{\omega}(t))$, where $\mathbf{R}(t)$ is a rotation matrix. The time dependence of $\boldsymbol{\eta} = [\boldsymbol{\eta}_1^T \ \ldots \ \boldsymbol{\eta}_N^T]^T, \boldsymbol{\psi}, \boldsymbol{\omega}$, and $\mathbf{R}$ will be omitted in the sequel for the sake of simplicity.

The following assumption is considered.

Assumption 1: The values of $\mathbf{R}(t)$ and $\boldsymbol{\omega}(t)$ are available to be used in the observer. Moreover, $\boldsymbol{\omega}(t)$ is bounded for all t, i.e.,

$$\exists_{0<W<\infty} \forall_t : \|\boldsymbol{\omega}(t)\| < W.$$

The problem under discussion in this section can be stated as follows.

Problem Statement: Consider the class of dynamic systems (1) verifying Assumption 1. Design a state observer that minimizes the impact of sensor noise and external disturbances on the state estimates.

B. Observer Design

This section presents the observer design for the class of systems introduced in Section II-A. First, the observer structure is imposed, leaving enough degrees of freedom to allow the design of a control mechanism to drive the observer error to zero. Afterwards, a coordinate transformation is applied to the resulting observer error dynamics that renders them LTI. The control of the observer error follows resorting to the standard $\mathcal{H}_\infty$ output feedback control synthesis technique, yielding the final observer dynamics.

Consider an observer with the following structure:

$$\begin{cases} \dot{\hat{\boldsymbol{\eta}}}_1 = \mathbf{f}_1 + \gamma_1 \hat{\boldsymbol{\eta}}_2 + \mathbf{S}(\boldsymbol{\omega})(\boldsymbol{\psi} - \hat{\boldsymbol{\eta}}_1) - \boldsymbol{\tau}_1 \\ \dot{\hat{\boldsymbol{\eta}}}_2 = \mathbf{f}_2 + \gamma_2 \hat{\boldsymbol{\eta}}_3 - \mathbf{S}(\boldsymbol{\omega})\hat{\boldsymbol{\eta}}_2 - \boldsymbol{\tau}_2 \\ \cdots \\ \dot{\hat{\boldsymbol{\eta}}}_{N-1} = \mathbf{f}_{N-1} + \gamma_{N-1}\hat{\boldsymbol{\eta}}_N - \mathbf{S}(\boldsymbol{\omega})\hat{\boldsymbol{\eta}}_{N-1} - \boldsymbol{\tau}_{N-1} \\ \dot{\hat{\boldsymbol{\eta}}}_N = \mathbf{f}_N - \mathbf{S}(\boldsymbol{\omega})\hat{\boldsymbol{\eta}}_N - \boldsymbol{\tau}_N \end{cases} \tag{2}$$

where

$$\boldsymbol{\tau}_i = \boldsymbol{\tau}_i(t, \boldsymbol{\omega}, \boldsymbol{\psi}, \hat{\boldsymbol{\eta}}), \quad i = 1, 2, \ldots, N$$

are virtual control variables that will be used to stabilize the observer error dynamics, with $\hat{\boldsymbol{\eta}} = [\hat{\boldsymbol{\eta}}_1^T \hat{\boldsymbol{\eta}}_2^T \ \ldots \ \hat{\boldsymbol{\eta}}_N^T]^T$. Notice that, apart from the output injection term $\mathbf{S}(\boldsymbol{\omega})(\boldsymbol{\psi} - \hat{\boldsymbol{\eta}}_1)$, this structure is an exact copy of the nominal system. The reasoning behind the introduction of this term will become clear later in this brief.

Let $\tilde{\boldsymbol{\eta}}_i = \boldsymbol{\eta}_i - \hat{\boldsymbol{\eta}}_i$, $i = 1, \ldots, N$, denote the state estimation errors. Hence, from (1) and (2), it follows that the observer error dynamics can be written as

$$\begin{cases} \dot{\tilde{\boldsymbol{\eta}}}_1 = \gamma_1 \tilde{\boldsymbol{\eta}}_2 - \mathbf{S}(\boldsymbol{\omega})\tilde{\boldsymbol{\eta}}_1 + \boldsymbol{\tau}_1 \\ \cdots \\ \dot{\tilde{\boldsymbol{\eta}}}_{N-1} = \gamma_{N-1}\tilde{\boldsymbol{\eta}}_N - \mathbf{S}(\boldsymbol{\omega})\tilde{\boldsymbol{\eta}}_{N-1} + \boldsymbol{\tau}_{N-1} \\ \dot{\tilde{\boldsymbol{\eta}}}_N = -\mathbf{S}(\boldsymbol{\omega})\tilde{\boldsymbol{\eta}}_N + \boldsymbol{\tau}_N \end{cases}$$

which are inherently time-varying. Next, this extra complexity is overcome through the use of an appropriate orthogonal time-varying coordinate transformation. To that purpose, define $\mathbf{x}_p = [\mathbf{x}_1^T \ \mathbf{x}_2^T \ \ldots \ \mathbf{x}_N^T]^T$ as

$$\mathbf{x}_p := \mathbf{T}(t)\tilde{\boldsymbol{\eta}} \tag{3}$$

where $\tilde{\boldsymbol{\eta}} = [\tilde{\boldsymbol{\eta}}_1^T \tilde{\boldsymbol{\eta}}_2^T \ \ldots \ \tilde{\boldsymbol{\eta}}_N^T]^T$ and $\mathbf{T}(t)$ is the coordinate transformation matrix defined as

$$\mathbf{T}(t) := \mathrm{diag}(\mathbf{R}, \ldots, \mathbf{R}).$$

Notice that (3) is a Lyapunov transformation [15] as follows:

- $\mathbf{T}(t)$ is continuous differentiable for all t;
- under Assumption 1 both $\mathbf{T}(t)$ and $\dot{\mathbf{T}}(t)$ are bounded for all t, where $\dot{\mathbf{T}}(t) = \mathbf{T}(t)\mathbf{M}_S(\boldsymbol{\omega})$, with $\mathbf{M}_S(\boldsymbol{\omega}) := \mathrm{diag}(\mathbf{S}(\boldsymbol{\omega}), \ldots, \mathbf{S}(\boldsymbol{\omega}))$;
- $\det[\mathbf{T}(t)] = 1$.

In the new coordinate space the observer error dynamics can be written as

$$\dot{\mathbf{x}}_p = \mathbf{A}_p\mathbf{x}_p + \mathbf{T}(t)\boldsymbol{\tau} \tag{4}$$

where

$$\mathbf{A}_p = \begin{bmatrix} \mathbf{0} & \gamma_1\mathbf{I} & \mathbf{0} & \ldots & \mathbf{0} \\ \vdots & \ddots & \ddots & \ddots & \vdots \\ \vdots & & \ddots & \ddots & \mathbf{0} \\ \vdots & & & \ddots & \gamma_{N-1}\mathbf{I} \\ \mathbf{0} & \ldots & \ldots & \ldots & \mathbf{0} \end{bmatrix}$$

and $\boldsymbol{\tau} = [\boldsymbol{\tau}_1^T\ \boldsymbol{\tau}_2^T\ \ldots\ \boldsymbol{\tau}_N^T]^T$. Applying the same coordinate transformation to the virtual control input of the observer error dynamics yields $\mathbf{u} = \mathbf{T}(t)\boldsymbol{\tau}$, that allows to rewrite (4) as

$$\dot{\mathbf{x}}_p = \mathbf{A}_p\mathbf{x}_p + \mathbf{u} \tag{5}$$

which is a linear time invariant system. Thus, with the coordinate transformation (3) the observer error dynamics are rendered LTI. The introduction of the term $\mathbf{S}(\boldsymbol{\omega})(\boldsymbol{\psi} - \hat{\boldsymbol{\eta}}_1)$ is now evident.

Naturally, not all the error states are available for feedback. In fact, and according to (1), only $\mathbf{x}_1$ is accessible. Thus, to complete the observer error dynamics, define as output

$$\mathbf{y}_p := \mathbf{C}_p\mathbf{x}_p \tag{6}$$

where $\mathbf{C}_p = [\mathbf{I}\,\mathbf{0}\ \ldots\ \mathbf{0}]$. Notice now that the LTI system (5)–(6) is both controllable and observable. Therefore, any control design methodology for linear time invariant systems can be employed to stabilize the observer error dynamics, in particular the $\mathcal{H}_\infty$ output feedback control synthesis. The employment of this design technique permits the natural use of frequency weights to shape both the exogenous and the internal signals. To that purpose, consider the block diagram depicted in Fig. 1, where the linear observer error dynamics are shown together with weight matrix transfer functions $\mathbf{W}_i(s)$, $i = 1, \ldots, 4$. In the figure, $\mathbf{w} = [\mathbf{w}_1^T\ \mathbf{w}_2^T]^T$ and $\mathbf{z} = [\mathbf{z}_1^T\ \mathbf{z}_2^T]^T$ represent the generalized disturbance and performance vectors, respectively. Notice that the models for the disturbance inputs and sensor noise live in the transformed space. The same applies to the performance weights.

Define $\mathbf{x} = [\mathbf{x}_p^T\,\mathbf{x}_{W1}^T\,\mathbf{x}_{W2}^T\,\mathbf{x}_{W3}^T\,\mathbf{x}_{W4}^T]^T$, where $\mathbf{x}_{Wi}, i = 1, \ldots, 4$, denotes the states of the state space realizations of the frequency weights $\mathcal{W}_i$, $i = 1, \ldots, 4$. Then, the augmented plant can be written, in a compact form, as

$$\begin{cases} \dot{\mathbf{x}} = \mathbf{A}\mathbf{x} + \mathbf{B}_1\mathbf{w} + \mathbf{B}_2\mathbf{u} \\ \mathbf{z} = \mathbf{C}_1\mathbf{x} + \mathbf{D}_{12}\mathbf{u} \\ \mathbf{y} = \mathbf{C}_2\mathbf{x} + \mathbf{D}_{21}\mathbf{w} \end{cases} \tag{7}$$

where the definition of the various matrices is omitted as it is evident from the context. The standard design setup and nomenclature in [16] is adopted and it is assumed that the $\mathcal{H}_\infty$ control problem is well-posed. Let $\mathbf{T}_{zw}(s)$ denote the closed-loop operator from the generalized disturbance vector $\mathbf{w}$ to the generalized performance vector $\mathbf{z}$. Then, the solution of the $\mathcal{H}_\infty$ output feedback control problem for the augmented plant (7) yields a stabilizing compensator

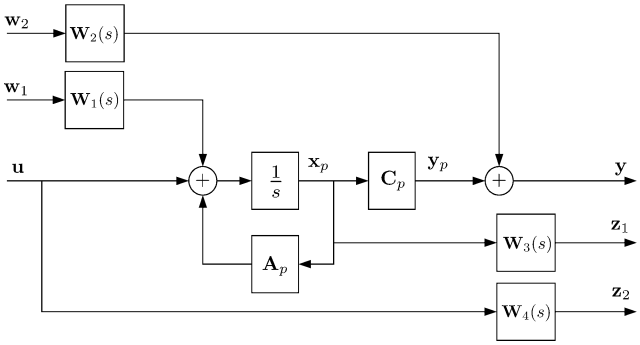

Fig. 1. Generalized LTI observer error dynamics.

$$\begin{cases} \dot{\mathbf{x}}_K = \mathbf{A}_K\mathbf{x}_K + \mathbf{B}_K\mathbf{y} \\ \mathbf{u} = \mathbf{C}_K\mathbf{x}_K \end{cases} \tag{8}$$

that minimizes $\|\mathbf{T}_{zw}(s)\|_\infty$. Combining (2) with (8) finally yields the time-varying realization of the observer in the original coordinates

$$\begin{cases} \dot{\hat{\boldsymbol{\eta}}} = \mathbf{f} + \mathbf{A}_p\hat{\boldsymbol{\eta}} - \mathbf{M}_S(\boldsymbol{\omega})\hat{\boldsymbol{\eta}} + \mathbf{C}_p^T\mathbf{S}(\boldsymbol{\omega})\boldsymbol{\psi} - [\mathbf{T}(t)]^T\mathbf{C}_K\mathbf{x}_K \\ \dot{\mathbf{x}}_K = \mathbf{A}_K\mathbf{x}_K + \mathbf{B}_K\mathbf{R}(\boldsymbol{\psi} - \hat{\boldsymbol{\eta}}_1) \end{cases} \tag{9}$$

where $\mathbf{f} = [\mathbf{f}_1^T\ \ldots\ \mathbf{f}_N^T]^T$.

C. Properties

In this section several properties of the proposed observer are presented and discussed. The proofs are presented in the appendix for the sake of readability. First, the asymptotic stability of the observer error dynamics is stressed in the following theorem.

Theorem 1: Consider the nominal dynamic system (1). Then, under Assumption 1, the error dynamics of the proposed time-varying observer (9) are globally exponentially stable.

The proposed observer is designed resorting to the $\mathcal{H}_\infty$ output feedback control methodology, which naturally displays a certain optimality property. In order to derive it, consider the generalized observer error dynamics depicted in Fig. 2. The main differences between this generalized plant and the one depicted in Fig. 1 are: 1) the generalized disturbances go through the transformation $\mathbf{T}^T(t)$ and 2) the generalized performance vector takes into account the system states and the control signal after the transformation $\mathbf{T}(t)$. In spite of these transformations, the magnitude of the signals is preserved—only the directionality is affected over time. Let $\boldsymbol{\chi} = [\tilde{\boldsymbol{\eta}}^T\,\mathbf{x}_{W1}^T\ \ldots\ \mathbf{x}_{W4}^T]^T$. Notice that $\boldsymbol{\chi} = \mathbf{T}_c^T(t)\mathbf{x}$, with dynamics given by

$$\dot{\boldsymbol{\chi}} = \boldsymbol{\mathcal{A}}(t)\boldsymbol{\chi} + \boldsymbol{\mathcal{B}}_1(t)\mathbf{w} + \boldsymbol{\mathcal{B}}_2(t)\boldsymbol{\tau}$$

where

$$\boldsymbol{\mathcal{A}}(t) = -\begin{bmatrix} \mathbf{M}_S(\boldsymbol{\omega}) & \mathbf{0} \\ \mathbf{0} & \mathbf{0} \end{bmatrix} + \mathbf{T}_c^T(t)\mathbf{A}\mathbf{T}_c(t)$$

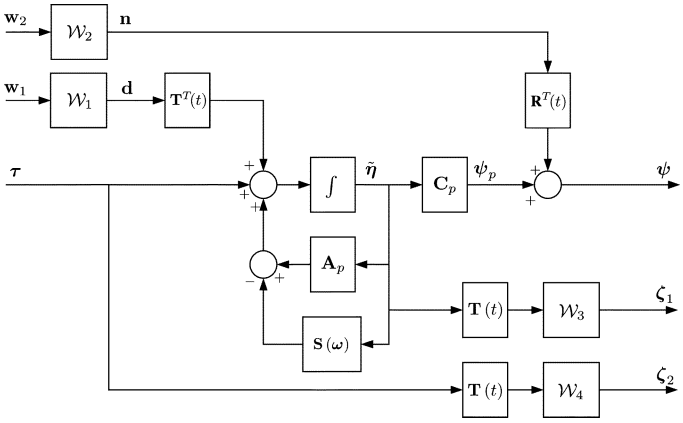

Fig. 2. Generalized observer error dynamics.

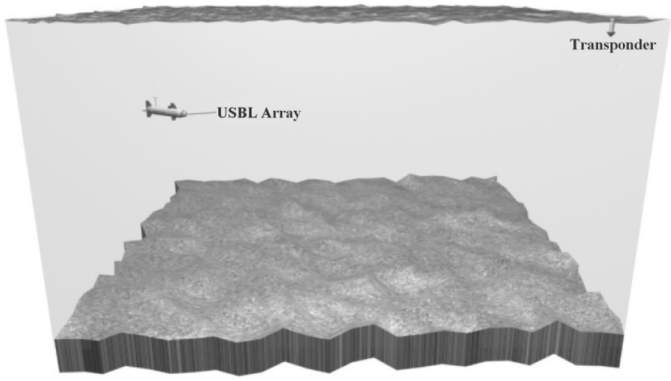

Fig. 3. Mission scenario.

$\boldsymbol{\mathcal{B}}_1(t) = \mathbf{T}_c^T(t)\mathbf{B}_1$, and $\boldsymbol{\mathcal{B}}_2(t) = \mathbf{T}_c^T(t)\mathbf{B}_2\mathbf{T}(t)$. The performance vector $\boldsymbol{\zeta} = [\boldsymbol{\zeta}_1^T\ \boldsymbol{\zeta}_2^T]^T$ can be written as

$$\boldsymbol{\zeta} = \boldsymbol{\mathcal{C}}_1(t)\boldsymbol{\chi} + \boldsymbol{\mathcal{D}}_{12}(t)\boldsymbol{\tau}$$

where $\boldsymbol{\mathcal{C}}_1(t) = \mathbf{C}_1\mathbf{T}_c(t)$ and $\boldsymbol{\mathcal{D}}_{12}(t) = \mathbf{D}_{12}\mathbf{T}(t)$. The generalized output is given by

$$\boldsymbol{\psi} = \boldsymbol{\mathcal{C}}_2(t)\boldsymbol{\chi} + \boldsymbol{\mathcal{D}}_{21}(t)\mathbf{w}$$

where $\boldsymbol{\mathcal{C}}_2(t) = \mathbf{R}^T(t)\mathbf{C}_2\mathbf{T}_c(t)$ and $\boldsymbol{\mathcal{D}}_{21}(t) = \mathbf{R}^T(t)\mathbf{D}_{21}$. The following theorem addresses the optimality of the proposed solution.

Theorem 2: Under the conditions of Theorem 1, the proposed observer minimizes the $\mathcal{L}_2$ induced norm from $\mathbf{w}$ to $\boldsymbol{\zeta}$, assuming that $\mathbf{w}$ is a finite energy signal, i.e., $\mathbf{w}$ is square integrable.

It is important to remark that the observer structure was previously imposed and did not arise naturally from the solution of an optimization problem. Nevertheless, good performance can be achieved by minimizing the $\mathcal{L}_2$ induced norm from $\mathbf{w}$ to $\boldsymbol{\zeta}$ in the augmented error dynamics depicted in Fig. 2, as it will be clearly demonstrated in the next section.

The exponential behavior of the observer error dynamics is a very important property. Nevertheless, there exist GES systems that, in the presence of disturbances, even arbitrarily small vanishing signals, are driven to infinity [17]. The following result characterizes the system with respect to perturbations in $\boldsymbol{\psi}, \mathbf{R}$, and $\boldsymbol{\omega}$.

Theorem 3: Suppose that $\boldsymbol{\psi}, \boldsymbol{\omega}$, and $\mathbf{R}$ in (9) are replaced by disturbed variables $\boldsymbol{\psi}_m = \boldsymbol{\psi} - \tilde{\boldsymbol{\psi}}, \boldsymbol{\omega}_m = \boldsymbol{\omega} - \tilde{\boldsymbol{\omega}}$, and $\mathbf{R}_m = \mathbf{R}[\mathbf{I} - \mathbf{S}(\tilde{\boldsymbol{\lambda}})]$, where $\tilde{\boldsymbol{\psi}}, \tilde{\boldsymbol{\omega}}$, and $\tilde{\boldsymbol{\lambda}}$ are the disturbances, respectively, and assume that the state $\boldsymbol{\eta}$ remains bounded for all time. Then, under the conditions of Theorem 1, the observer error is locally ISS, with $[\tilde{\boldsymbol{\psi}}^T, \tilde{\boldsymbol{\omega}}^T, \tilde{\boldsymbol{\lambda}}^T]^T$ as input.

III. Position and Current Observer

A. Problem Statement

The application detailed in this brief revisits the problem described in [14]. Consider an underwater vehicle equipped with an acoustic positioning system like an ultra-short baseline (USBL) sensor and suppose that there is a moored buoy in the mission scenario where an acoustic transponder is installed. Fig. 3 depicts the scenario just described. The linear motion kinematics of the vehicle can be written as

$$\dot{\mathbf{p}} = \mathbf{R}\mathbf{v}$$

where $\mathbf{p}$ is the position of the origin of the body-fixed coordinate system $\{B\}$ described in the inertial coordinate system $\{I\}$, $\mathbf{R}$ is the rotation matrix from $\{B\}$ to $\{I\}$, that verifies $\dot{\mathbf{R}} = \mathbf{R}\mathbf{S}(\boldsymbol{\omega})$, $\mathbf{v}$ is the linear velocity of the vehicle relative to $\{I\}$, expressed in body-fixed coordinates, and $\boldsymbol{\omega}$ is the vehicle angular velocity, also expressed in body-fixed coordinates. Assume that the buoy where the transponder is installed is subject to wave action of known power spectral density that affects its position over time, and suppose that the position of the transponder with respect to the vehicle is available, in body-fixed coordinates as measured by the USBL sensor installed on-board. Suppose also that the body angular velocity $\boldsymbol{\omega}$ and the rotation matrix $\mathbf{R}$ are available from an Attitude and Heading Reference System (AHRS). Finally, suppose that the vehicle is moving in deep waters (far from the wave action), in the presence of an ocean current of constant unknown velocity, which expressed in body-fixed coordinates is represented by $\mathbf{v}_c$.

The problem considered here is that of estimate the velocity of the current and the position of the transponder with respect to the vehicle. Further consider that the velocity of the vehicle relative to the water is available from the measures of an on-board Doppler velocity log. In shallow waters, this sensor can be employed to measure both the velocity of the vehicle relative to the inertial frame and relative to the water. However, when the vehicle is far from the seabed the inertial velocity is usually unavailable. By estimating the ocean current velocity, an estimate of the velocity of the vehicle relative to the inertial frame is immediately obtained.

B. Proposed Solution

Let $\mathbf{e}$ denote the position of the transponder relative to $\{B\}$ and $\mathbf{v}_r$ denote the velocity of the vehicle relative to the fluid, both expressed in body-fixed coordinates. Since the transponder is assumed at rest (in the absence of environmental disturbances) in the inertial frame, the time derivative of $\mathbf{e}$ is given by

$$\dot{\mathbf{e}} = -\mathbf{v}_r - \mathbf{v}_c - \mathbf{S}(\boldsymbol{\omega})\mathbf{e}. \tag{10}$$

On the other hand, as the velocity of the fluid is assumed to be constant in the inertial frame, the time derivative of this quantity expressed in body-fixed coordinates is simply given by

$$\dot{\mathbf{v}}_c = -\mathbf{S}(\boldsymbol{\omega})\mathbf{v}_c. \tag{11}$$

Notice that the vehicle velocity relative to the inertial frame satisfies $\mathbf{v} = \mathbf{v}_r + \mathbf{v}_c$.

Clearly, the problem of estimating the velocity of the fluid $\mathbf{v}_c$ falls into the class of problems addressed in the brief, with $\boldsymbol{\eta}_1 = \mathbf{e}, \boldsymbol{\eta}_2 = \mathbf{v}_c, \gamma_1 = -1$

$$\mathbf{f}_1 = -\mathbf{v}_r - \mathbf{S}(\boldsymbol{\omega})\mathbf{e},$$
$$\mathbf{f}_2 = \mathbf{0}$$

and $N = 2$. Thus, it is possible to design an observer as detailed in Section II. The simplicity of the model (10)–(11) arises from the fact that the linear motion of the vehicle is expressed by a pure kinematic description, which is exact and has been widely used by the scientific community in the design of aided Navigation Systems. The novelty of the proposed solution arises from expressing the rigid-body kinematics in body-fixed coordinates, which allows the derivation of (10)–(11).

Note that, in this case, the position of the transponder changes with time as the latter is assumed to be mounted in a buoy moored close to the sea surface, subject to strong wave action. Nevertheless, the buoy wave induced random motion can be modeled as an external disturbance on the USBL positioning system expressed on the inertial frame, and its description embedded in the frequency weights as presented in Section II. As closed-loop design objective consider the rejection of the induced wave disturbances from the position measurements to the position and current velocity estimates, as well as the noise in the position and relative velocity measurements.

The disturbances induced by the 3-D wave random field in the position of the buoy are modeled using three second-order harmonic oscillators representing the disturbance models along the x, y, and z directions,

$$H_w^i(s) = \frac{\sigma_i s}{s^2 + 2\xi_i\omega_{0i}s + \omega_{0i}^2}, \quad i = 1, 2, 3$$

where ω_{0i} is the dominating wave frequency along each axis, ξ_i is the relative damping ratio, and σ_i is a parameter related to the wave intensity, see [3] and [18] for further details. The sensor frequency weight matrix transfer function $\mathbf{W}_2(s)$ was chosen as

$$\mathbf{W}_2(s) = 5\left(1 + \frac{\sigma_i s}{s^2 + 2\xi_i\omega_{0i}s + \omega_{0i}^2}\right)\mathbf{I}_3.$$

Notice that a direct term was included, not only to satisfy design requirements (nonzero sensor noise), but also to model the noise on the USBL, which was assumed Gaussian with standard deviation of 1 m. In the simulation, the dominating wave frequency was set to $\omega_{0i} = 0.90$ rad/s and the relative damping ratio to $\xi_i = 0.1$.

Although there is no model uncertainty, as the observer nominal model that corresponds to the kinematics of the linear motion is exact, the weight $\mathbf{W}_1(s)$ was set to $\mathbf{W}_1(s) = 0.01\mathbf{I}_6$ to model possible state disturbances steaming, e.g., from the relative velocity sensor. Since this is a pure disturbance rejection control problem, the performance weights were selected as $\mathbf{W}_3(s) = \mathbf{I}_6$. Finally, the virtual control input weights were chosen as $\mathbf{W}_4(s) = 2(s+1)/(s+10)\mathbf{I}_6$ to properly tune the input-output behavior of the closed-loop system.

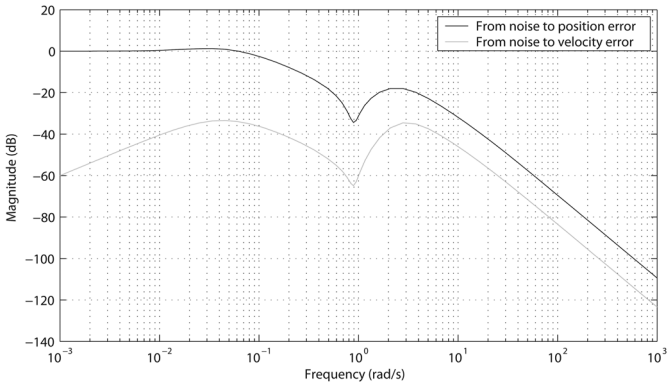

Fig. 4. Singular values of the closed-loop system.

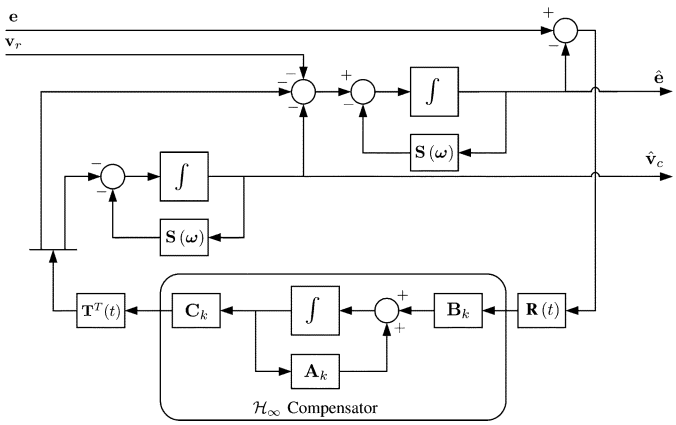

Fig. 5. Position and current velocity observer block diagram implementation.

Fig. 4 shows the singular values of the linear closed-loop transfer functions from the position error measurements in the inertial frame, signal $\mathbf{n}$ in Fig. 2, to the position and current velocity estimate errors in the inertial frame, $\mathbf{R}\tilde{\mathbf{e}}$ and $\mathbf{R}\tilde{\mathbf{v}}_c$, respectively. The diagram shows that the performance requirements are met by the resultant closed loop system, which is evident from the band rejection characteristics of the notch present in both singular value diagrams.

The structure of the resulting observer is depicted in Fig. 5, where the H_∞ output feedback compensator is of order 18.

C. Simulation Results

To illustrate the performance of the proposed solution a simulation was carried out with the observer installed on-board the underwater vehicle SIRENE, see [19].

In addition to the disturbances induced by ocean waves and the noise on the USBL positioning system, in the simulation the measurements of the vehicle velocity relative to the water were also assumed to be corrupted by Gaussian noise with standard deviations of 0.01 m/s. The AHRS was assumed to provide the roll, pitch, and yaw Euler angles, corrupted by Gaussian noises with standard deviation of 0.03° for the roll and pitch and 0.3°

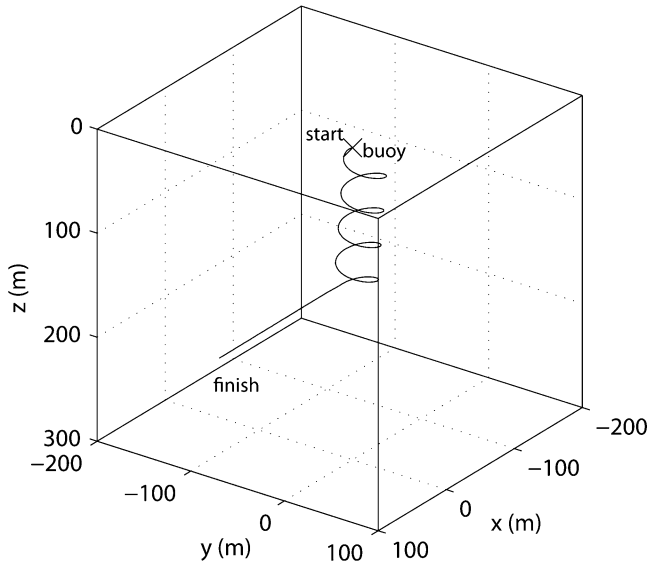

Fig. 6. Trajectory described by the vehicle.

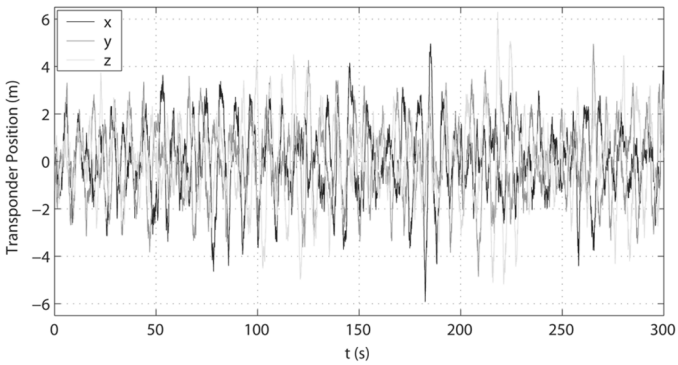

Fig. 7. Time evolution of the position of the buoy (in the inertial frame).

for the yaw, and the angular velocity corrupted with Gaussian noise with standard deviation of 0.02 °/s.

The trajectory described by the vehicle is shown in Fig. 6 and the actual position of the buoy, expressed in the inertial frame, is depicted in Fig. 7. As it can be seen, the buoy wave induced random motion is confined to intervals of about 10 m of amplitude, which corresponds to extreme weather conditions.

The observer was initialized with zero on all estimates but the position of the buoy, which was initialized with the first measurement provided by the USBL positioning sensor. The time evolution of the observer estimates is presented in Figs. 8 and 9. The position of the buoy if there were no ocean waves is also shown, as well as the actual velocity of the fluid, all expressed in body-fixed coordinates. From these plots the performance of the observer is evident—only the initial transients are noticeable. Since the observer works in body-fixed coordinates, the estimate of the ocean current changes with the attitude of the vehicle. In order to better evaluate the results, Fig. 10 presents the evolution of the estimate of the ocean current transformed back to the inertial frame. Clearly, the observer estimate converges to the actual value of the ocean current, which was set in the simulation to $[1 \; -2 \; 0.5]^T$ (m).

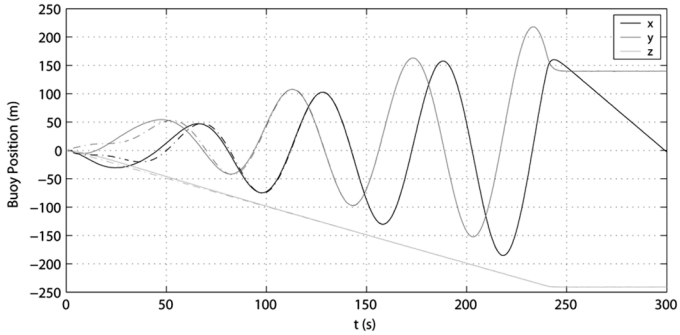

Fig. 8. Actual (dashed-dotted lines) and estimated (solid lines) buoy position.

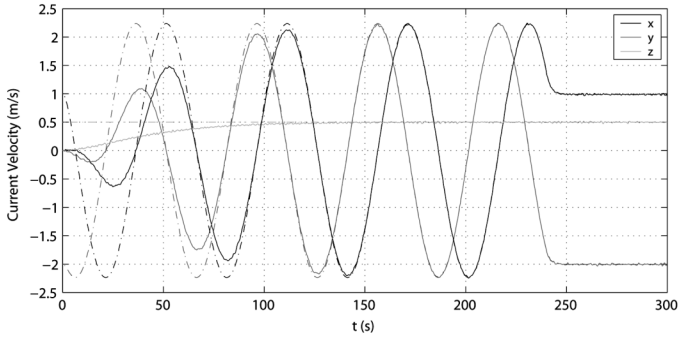

Fig. 9. Actual (dashed-dotted lines) and estimated (solid lines) ocean current velocity.

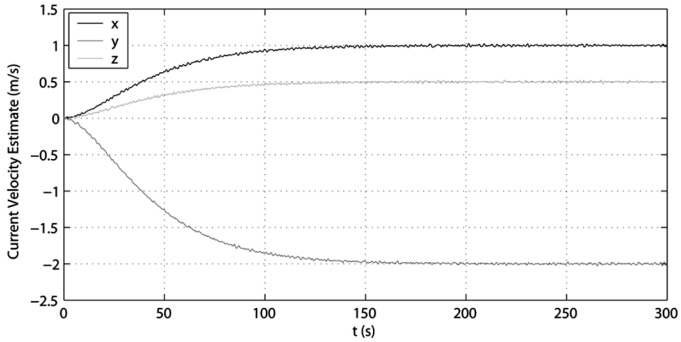

Fig. 10. Ocean current velocity estimate in inertial coordinates.

The evolution of the observer error variables is shown in Fig. 11. The initial transients arise due to the mismatch of the initial conditions of the states of the observer and can be considered as a warming up time of 180 s of the corresponding Integrated Navigation System. The observer error variables are shown in greater detail in Fig. 12. From the various plots it can be concluded that the disturbances induced by the waves, as well as the sensors' noise, are highly attenuated by the observer, producing very accurate estimates of the velocity of the current and the position of the buoy.

The estimated trajectory of the buoy, as seen from the vehicle, that is, expressed in body-fixed coordinates, is depicted in Fig. 13(a), where the trajectory that would be described by the buoy at rest is also shown. For comparison purposes, the non-filtered position of the buoy as measured by the USBL sensor is plotted in Fig. 13(b). Once again, the figures clearly show the performance achieved by the proposed solution.

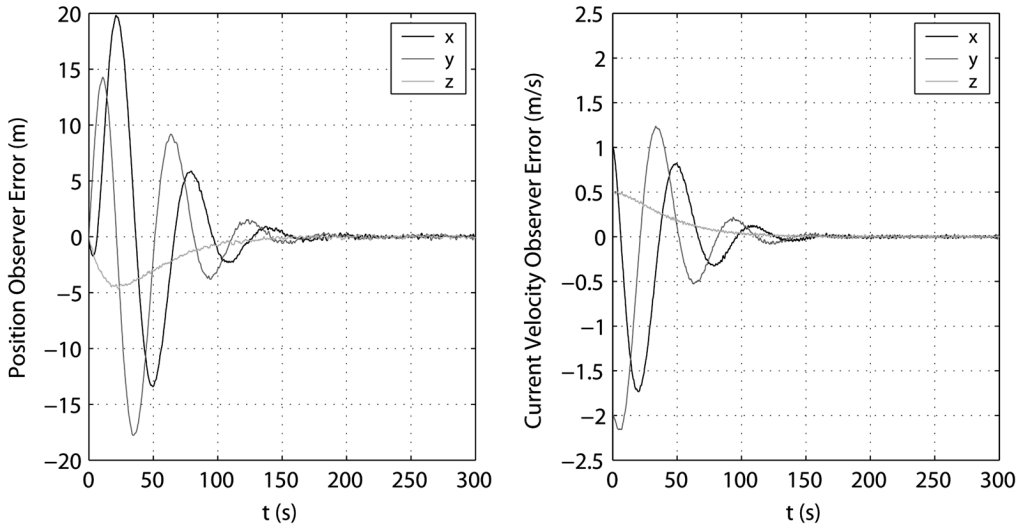

Fig. 11. Time evolution of the observer error variables.

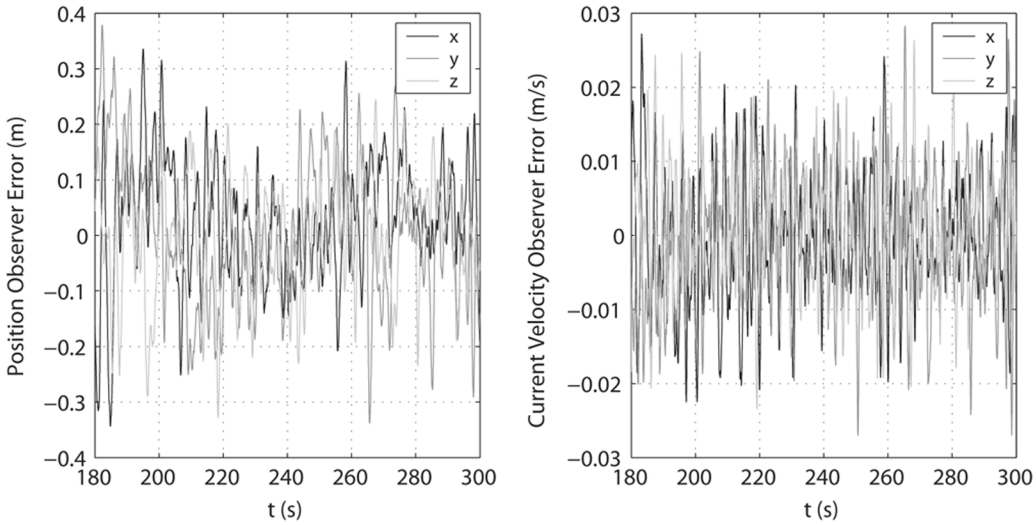

Fig. 12. Detailed evolution of the observer error variables.

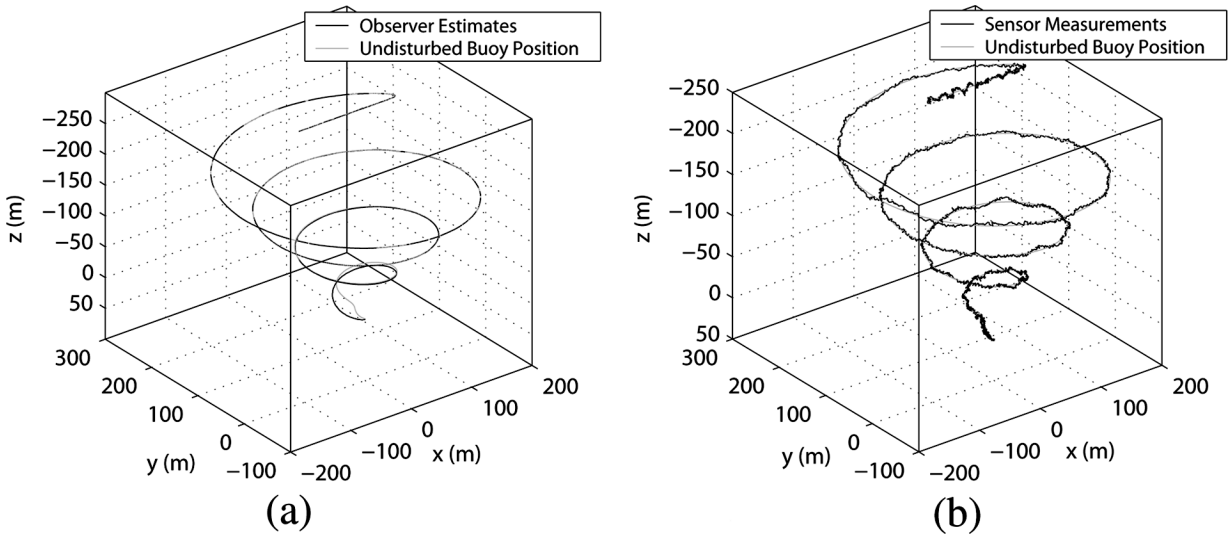

Fig. 13. Trajectory of the buoy as seen from the vehicle. (a) Estimated trajectory. (b) Non-filtered trajectory.

IV. Conclusion

This brief presented an observer design methodology for a class of kinematic systems with particular application to the estimation of linear quantities (position, linear velocity, and ocean current) in Integrated Navigation Systems. At the core of the proposed methodology there is a time-varying orthog-

onal coordinate transformation that renders the observer error dynamics LTI. The problem was then formulated as a virtual control problem which was solved by resorting to the standard $\mathcal{H}_\infty$ output feedback control synthesis technique, thus minimizing the $\mathcal{L}_2$ induced norm from a generalized disturbance input to a performance variable. The resulting observer error dynamics are GES and ISS with respect to the variables of interest. A case study of practical interest in marine applications was presented that demonstrates the potential and usefulness of the proposed observer design methodology. Simulation results were offered that illustrate the achievable performance in the presence of extreme environmental disturbances and realistic measurement noise. Other applications can be devised in the design of navigation systems for other mobile platforms such as aerospace or ground vehicles.

APPENDIX
PROOFS

Proof of Theorem 1: It has been established before that, with the proposed observer design, the closed-loop observer error dynamics in the transformed coordinate space are globally asymptotically stable and, since they are linear time invariant, the convergence is exponentially fast. Now, using the fact that a Lyapunov coordinate transformation is employed, it follows that the original observer error, $\tilde{\boldsymbol{\eta}}$, also converges exponentially fast to zero [15].

Remark 1: The previous result can also be established using the Lyapunov function

$$V := \left[\tilde{\boldsymbol{\eta}}^T \, \mathbf{x}_K^T\right] \mathbf{P}(t) \left[\tilde{\boldsymbol{\eta}}^T \, \mathbf{x}_K^T\right]^T \tag{12}$$

with

$$\mathbf{P}(t) := \mathbf{T}_c^T(t) \mathbf{P}_0 \mathbf{T}_c(t)$$

where

$$\mathbf{T}_c(t) := \operatorname{diag}(\mathbf{T}(t), \mathbf{I})$$

and $\mathbf{P}_0$ is the positive definite solution of the Lyapunov equation

$$\mathbf{A}_c^T \mathbf{P}_0 + \mathbf{P}_0 \mathbf{A}_c = -\mathbf{I}$$

where

$$\mathbf{A}_c = \begin{bmatrix} \mathbf{A}_p & \mathbf{C}_K \\ \mathbf{B}_K \mathbf{C}_p & \mathbf{A}_K \end{bmatrix}.$$

Proof of Theorem 2: Suppose that $\mathbf{w} \in \mathcal{L}_2$, where $\mathcal{L}_2$ denotes the set of real-valued finite energy signals, and consider the closed-loop systems from $\mathbf{w}$ to $\mathbf{z}$ and from $\mathbf{w}$ to $\boldsymbol{\zeta}$. Let γ^*, associated to the control input $\boldsymbol{\tau}^*(t)$, be the minimum γ that satisfies

$$\int \boldsymbol{\zeta}^T(t) \boldsymbol{\zeta}(t) \, dt \leq \gamma^2 \int \mathbf{w}^T(t) \mathbf{w}(t) \, dt$$

and γ_l^*, associated with the control input $\mathbf{u}^*(t)$, be the minimum γ_l that satisfies

$$\int \mathbf{z}^T(t) \mathbf{z}(t) \, dt \leq \gamma_l^2 \int \mathbf{w}^T(t) \mathbf{w}(t) \, dt.$$

Notice that $\mathbf{u}^*(t)$ is the control signal resulting from the $\mathcal{H}_\infty$ output feedback control synthesis.

Choosing $\boldsymbol{\tau}(t) = \mathbf{T}^T(t) \mathbf{u}^*(t)$, it is easy to show that

$$\int \boldsymbol{\zeta}^T(t) \boldsymbol{\zeta}(t) \, dt = \int \mathbf{z}^T(t) \mathbf{z}(t) \, dt \Bigg|_{\substack{\mathbf{u}(t) = \mathbf{u}^*(t) \\ \boldsymbol{\tau}(t) = \mathbf{T}^T(t) \mathbf{u}^*(t)}}.$$

Since

$$\int \mathbf{z}^T(t) \mathbf{z}(t) \, dt \leq \gamma_l^* \int \mathbf{w}^T(t) \mathbf{w}(t) \, dt \Big|_{\mathbf{u}(t) = \mathbf{u}^*(t)}$$

it is immediate that

$$\int \boldsymbol{\zeta}^T(t) \boldsymbol{\zeta}(t) \, dt \leq \gamma_l^* \int \mathbf{w}^T(t) \mathbf{w}(t) \, dt \Big|_{\boldsymbol{\tau}(t) = \mathbf{T}^T(t) \mathbf{u}^*(t)}.$$

from which one concludes that $\gamma^* \leq \gamma_l^*$. On the other hand, choosing $\mathbf{u}(t) = \mathbf{T}(t) \boldsymbol{\tau}^*(t)$, it is easy to show that

$$\int \mathbf{z}^T(t) \mathbf{z}(t) \, dt = \int \boldsymbol{\zeta}^T(t) \boldsymbol{\zeta}(t) \, dt \Bigg|_{\substack{\mathbf{u}(t) = \mathbf{T}(t) \boldsymbol{\tau}^*(t) \\ \boldsymbol{\tau}(t) = \boldsymbol{\tau}^*(t)}}.$$

Since

$$\int \boldsymbol{\zeta}^T(t) \boldsymbol{\zeta}(t) \, dt \leq \gamma^* \int \mathbf{w}^T(t) \mathbf{w}(t) \, dt \Big|_{\boldsymbol{\tau}(t) = \boldsymbol{\tau}^*(t)}$$

it is immediate that

$$\int \mathbf{z}^T(t) \mathbf{z}(t) \, dt \leq \gamma^* \int \mathbf{w}^T(t) \mathbf{w}(t) \, dt \Big|_{\mathbf{u}(t) = \mathbf{T}(t) \boldsymbol{\tau}^*(t)}$$

from which one concludes that $\gamma_l^* \leq \gamma^*$. Since $\gamma^* \leq \gamma_l^*$ and $\gamma_l^* \leq \gamma^*$ it must be $\gamma^* = \gamma_l^*$ with $\boldsymbol{\tau}^*(t) = \mathbf{T}^T(t) \mathbf{u}^*(t)$. Thus, the proposed time-varying observer minimizes the $\mathcal{L}_2$ induced norm from $\mathbf{w}$ to $\boldsymbol{\zeta}$.

Proof of Theorem 3: Suppose that $\boldsymbol{\psi}, \boldsymbol{\omega}$, and $\mathbf{R}$ in (9) are replaced by disturbed variables $\boldsymbol{\psi}_m = \boldsymbol{\psi} - \tilde{\boldsymbol{\psi}}$, $\boldsymbol{\omega}_m = \boldsymbol{\omega} - \tilde{\boldsymbol{\omega}}$, and $\mathbf{R}_m = \mathbf{R}[\mathbf{I} - \mathbf{S}(\tilde{\boldsymbol{\lambda}})]$, where $\tilde{\boldsymbol{\psi}}, \tilde{\boldsymbol{\omega}}$, and $\tilde{\boldsymbol{\lambda}}$ are the disturbances, respectively. Then, the dynamics of the observer can be written as

$$\begin{cases} \dot{\hat{\boldsymbol{\eta}}} = \mathbf{f} + \mathbf{A}_p \hat{\boldsymbol{\eta}} - \mathbf{M}_S(\boldsymbol{\omega} - \tilde{\boldsymbol{\omega}}) \hat{\boldsymbol{\eta}} + \mathbf{C}_p^T \mathbf{S}(\boldsymbol{\omega} - \tilde{\boldsymbol{\omega}})(\boldsymbol{\psi} - \tilde{\boldsymbol{\psi}}) \\ \qquad\qquad - (\mathbf{T}(t)[\mathbf{I} - \mathbf{M}_S(\tilde{\boldsymbol{\lambda}})])^T \mathbf{C}_K \mathbf{x}_K \\ \dot{\mathbf{x}}_K = \mathbf{A}_K \mathbf{x}_K + \mathbf{B}_K \mathbf{R}[\mathbf{I} - \mathbf{S}(\tilde{\boldsymbol{\lambda}})](\boldsymbol{\psi} - \hat{\boldsymbol{\eta}}_1 - \tilde{\boldsymbol{\psi}}) \end{cases}$$

and the error dynamics as

$$\begin{cases} \dot{\tilde{\boldsymbol{\eta}}} = \mathbf{A}_p \tilde{\boldsymbol{\eta}} - \mathbf{M}_S(\boldsymbol{\omega}) \tilde{\boldsymbol{\eta}} + [\mathbf{T}(t)]^T \mathbf{C}_K \mathbf{x}_K \\ \quad + \mathbf{C}_p^T \mathbf{S}(\boldsymbol{\omega}) \tilde{\boldsymbol{\psi}} + \mathbf{C}_p^T \mathbf{S}(\tilde{\boldsymbol{\omega}})(\boldsymbol{\psi} - \tilde{\boldsymbol{\psi}}) \\ \quad - \mathbf{M}_S(\tilde{\boldsymbol{\omega}})(\boldsymbol{\eta} - \tilde{\boldsymbol{\eta}}) + \mathbf{M}_S(\tilde{\boldsymbol{\lambda}})[\mathbf{T}(t)]^T \mathbf{C}_K \mathbf{x}_K \\ \dot{\mathbf{x}}_K = \mathbf{A}_K \mathbf{x}_K + \mathbf{B}_K \mathbf{R}(t) \tilde{\boldsymbol{\eta}}_1 \\ \quad - \mathbf{B}_K \mathbf{R} \mathbf{S}(\tilde{\boldsymbol{\lambda}}) \tilde{\boldsymbol{\eta}}_1 - \mathbf{B}_K \mathbf{R}[\mathbf{I} - \mathbf{S}(\tilde{\boldsymbol{\lambda}})] \tilde{\boldsymbol{\psi}} \end{cases}$$

or, in a compact form, as

$$\begin{bmatrix} \dot{\tilde{\boldsymbol{\eta}}} \\ \dot{\mathbf{x}}_K \end{bmatrix} = \mathbf{F}(t, \tilde{\boldsymbol{\eta}}, \mathbf{x}_K, \tilde{\boldsymbol{\psi}}, \tilde{\boldsymbol{\lambda}}, \tilde{\boldsymbol{\omega}}) \begin{bmatrix} \tilde{\boldsymbol{\eta}} \\ \mathbf{x}_K \end{bmatrix} \tag{13}$$

where the definition of $\mathbf{F}(t, \tilde{\boldsymbol{\eta}}, \mathbf{x}_K, \tilde{\boldsymbol{\psi}}, \tilde{\boldsymbol{\lambda}}, \tilde{\boldsymbol{\omega}})$ follows from the context. This function is continuously differentiable and, assuming that $\boldsymbol{\eta}$ remains bounded for all t, and as $\boldsymbol{\omega}(t)$ is

also assumed to be a bounded function of t, it follows that, in some neighborhood of the origin, the Jacobian matrices $[\partial \mathbf{F}/\partial(\tilde{\boldsymbol{\eta}}, \mathbf{x}_K)]$ and $[\partial \mathbf{F}/\partial(\tilde{\boldsymbol{\psi}}, \tilde{\boldsymbol{\lambda}}, \tilde{\boldsymbol{\omega}})]$ are bounded, uniformly in t. Since, in addition to that, the system

$$\begin{bmatrix} \dot{\tilde{\boldsymbol{\eta}}} \\ \dot{\mathbf{x}}_K \end{bmatrix} = \mathbf{F}(t, \tilde{\boldsymbol{\eta}}, \mathbf{x}_K, \mathbf{0}, \mathbf{0}, \mathbf{0}) \begin{bmatrix} \tilde{\boldsymbol{\eta}} \\ \mathbf{x}_K \end{bmatrix}$$

has a uniformly asymptotically stable equilibrium point at the origin, then (13) is locally input-to-state stable with $[\tilde{\boldsymbol{\psi}}^T, \tilde{\boldsymbol{\omega}}^T, \tilde{\boldsymbol{\lambda}}^T]^T$ as input [20, Lemma 5.4].

REFERENCES

[1] T. Fossen and A. Grøvlen, "Nonlinear output feedback control of dynamically positioned ships using vectorial observer backstepping," *IEEE Trans. Control Syst. Technol.*, vol. 6, no. 1, pp. 121–128, Jan. 1998.

[2] A. Robertsson and R. Johansson, "Comments on 'Nonlinear output feedback control of dynamically positioned ships using vectorial observer backstepping'," *IEEE Trans. Control Syst. Technol.*, vol. 6, no. 3, pp. 439–441, May 1998.

[3] T. I. Fossen and J. P. Strand, "Passive nonlinear observer design for ships using Lyapunov methods: Full-scale experiments with a supply vessel," *Automatica*, vol. 35, no. 1, pp. 3–16, Jan. 1999.

[4] *New Directions in Nonlinear Observer Design (Lecture Notes in Control and Information Sciences)*, H. Nijmeijer and T. I. Fossen, Eds. New York: Springer, 1999.

[5] A. Pascoal, I. Kaminer, and P. Oliveira, "Navigation system design using time varying complementary filters," *IEEE Aerosp. Electron. Syst.*, vol. 36, no. 4, pp. 1099–1114, Oct. 2000.

[6] H. Berghuis and H. Nijmeijer, "A passivity approach to controller-observer design for robots," *IEEE Trans. Robot. Autom.*, vol. 9, no. 6, pp. 740–754, Dec. 1993.

[7] C. De Wit and J.-J. Slotine, "Sliding observers for robot manipulators," *Automatica*, vol. 27, no. 5, pp. 859–864, 1991.

[8] R. Skjetne and H. Shim, "A systematic nonlinear observer design for a class of Euler-Lagrange systems," presented at the 9th Mediterranean Conf. Control Autom., Dubrovnik, Croatia, Jun. 2001.

[9] R. Ortega, A. Loria, P. J. Nicklasson, and H. Sira-Ramirez, *Passivity-Based Control of Euler-Lagrange Systems: Mechanical, Electrical and Electromechanical Applications*. New York: Springer, 1998.

[10] J. E. Refsnes, A. Sørensen, and K. Y. Pettersen, "Robust observer design for underwater vehicles," presented at the 46th IEEE Conf. Control Appl., Munich, Germany, Oct. 2006.

[11] J. Kinsey and L. Whitcomb, "Model-based nonlinear observers for underwater vehicle navigation: Theory and preliminary experiments," in *Proc. IEEE Int. Conf. Robot. Autom.*, Rome, Italy, Apr. 2007, pp. 4251–4256.

[12] P. G. Savage, "Strapdown inertial navigation integration algorithm design Part 2: Velocity and position algorithms," *J. Guid., Control, Dyn.*, vol. 21, no. 2, pp. 208–221, Mar. 1998.

[13] P. Batista, C. Silvestre, and P. Oliveira, "Observer design for a class of kinematic systems," presented at the 46th IEEE Conf. Decision Control, New Orleans, LA, Dec. 2007.

[14] P. Batista, C. Silvestre, and P. Oliveira, "A quaternion sensor based controller for homing of underactuated AUVs," in *Proc. 45th IEEE Conf. Dec. Control*, San Diego, CA, Dec. 2006, pp. 51–56.

[15] R. W. Brockett, *Finite Dimensional Linear Systems*. New York: Wiley, 1970.

[16] K. Zhou, J. C. Doyle, and K. Glover, *Robust and Optimal Control*. Englewood Cliffs, NJ: Prentice-Hall, 1995.

[17] A. R. Teel and J. Hespanha, "Examples of GES systems that can be driven to infinity by arbitrarily small additive decaying exponentials," *IEEE Trans. Autom. Control*, vol. 49, no. 8, pp. 1407–1410, Aug. 2004.

[18] C. Silvestre, A. Pascoal, and A. Healey, "AUV control under wave disturbances," in *Proc. 10th Int. Symp. Unmanned Untethered Vehicle Technol.*, Durham, New Hampshire, Sep. 1997, pp. 228–239.

[19] C. Silvestre, A. Aguiar, P. Oliveira, and A. Pascoal, "Control of the SIRENE underwater shuttle: System design and tests at sea," presented at the 17th Int. Conf. Offshore Mechan. Artie Eng. (OMAE-Conf.), Lisboa, Portugal, Jul. 1998.

[20] H. K. Khalil, *Nonlinear Systems*, 2nd ed. Englewood Cliffs, NJ: Prentice-Hall, 1996.